Plant Physiology and Biochemistry 142 (2019) 303–311

Contents lists available at ScienceDirect

Plant Physiology and Biochemistry

journal homepage: www.elsevier.com/locate/plaphy

Research article

The barley miR393 has multiple roles in regulation of seedling growth, stomatal density, and drought stress tolerance

Weiyi Yuan, Jingqi Suo, Bo Shi, Chenlu Zhou, Bin Bai, Hongwu Bian, Muyuan Zhu, Ning Han*

Key Laboratory for Cell and Gene Engineering of Zhejiang Province, Institute of Genetics and Regenerative Biology, College of Life Sciences, Zhejiang University, Hangzhou, 310058, Zhejiang, China

ARTICLE INFO

Keywords:
miR393
Auxin response
Stomata
Drought tolerance
Barley

ABSTRACT

microRNA393 (miR393) and its target module have been implicated as comprising a conserved mechanism to regulate developmental processes and plant growth in response to environmental signals through the auxin signaling pathway. Our previous work identified miR393 and its two targets in barley. In this study, we further investigated the expression pattern of miR393 and its biological functions in seedling growth and drought tolerance. We showed that the miR393 overexpressing line (*OE*) exhibited increased stomatal density with decreased guard cell length, while the miR393 knockdown line (*MIM*) displayed the opposite phenotype, which might be due to the effects of miR393 on *AUXIN RESPONSE FACTOR5* (*ARF5*) and three stomatal development-related genes, such as *EPIDERMAL PATTERNING FACTOR1* (*EPF1*), *SPEECHLESS* (*SPCH*), and *MUTE*. In addition, the *MIM* line conferred enhanced drought tolerance, with alleviated leaf chlorosis and lipid peroxidation after 22 days drought treatment. In contrast, the *OE* line was more sensitive to drought stress and accumulated more malondialdehyde and hydrogen peroxide than the wild type. Furthermore, polyethylene glycol (PEG) treatment-induced abscisic acid (ABA) accumulation in leaves was suppressed in the *OE* line, indicating that miR393 might regulate drought stress response and tolerance through its interaction with ABA biosynthesis. Overall, these data suggest that miR393 might be a potential target for manipulation of stomatal density and improvement of drought tolerance in barley.

1. Introduction

Since its discovery as a substance regulating phototropism, auxin has been implicated in diverse physiological processes in plants, including root gravitropism, lateral root development, leaf and vein development and shoot apical meristem activity. The effects of auxin depend upon its biosynthesis, transport, perception, signaling, and target gene responses. Most of these functions are controlled by a series of transcription factors with different cell specificities, and/or by cooperating directly or indirectly with other hormones (Kieffer et al., 2010).

MicroRNAs (miRNAs) are short, ~21-nucleotide-long, non-coding RNAs with essential functions in regulating gene expression in plants and animals (Voinnet, 2009). Previous studies have demonstrated that some genes encoding AUXIN RESPONSE FACTORS (ARFs) are under miRNA-mediated post-transcriptional regulation (Williams et al., 2005). For examples, miR160 targets *ARF10* to regulate seed germination and post-embryonic developmental programs in *Arabidopsis thaliana* (Liu et al., 2007), and promotes nodule formation and maturation in soybean (Nizampatnam et al., 2015). Another miRNA, miR167, is required for nodulation and lateral root development through targeting *GmARF8a* and *GmARF8b* in soybean (Wang et al., 2015), and regulates both female and male reproduction in *Arabidopsis* (Wu et al., 2006). The third group of *ARFs*, such as *ARF2*, *ARF3*, and *ARF4*, are controlled by trans-acting short interfering RNA3 (TAS3)-derived trans-acting small interfering RNAs; the latter are produced by miR390-mediated cleavage of the *TAS3* transcript (Marin et al., 2010). The miR390/*TAS3*/*ARF* module participates in leaf patterning and expansion, developmental phase transition, shoot meristem initiation, lateral root (LR) growth, nodule symbiosis, and gall formation (Cabrera et al., 2016; Hobecker et al., 2017; Marin et al., 2010).

Abbreviations: microRNA, miRNA; AUXIN RESPONSE FACTORS, ARFs; EPIDERMAL PATTERNING FACTOR, EPF; SPEECHLESS, SPCH; lateral root, LR; trans-acting short interfering RNA, TAS; Skp1-Cullin1-F-box protein, SCF; TRANSPORT INHIBITOR RESPONSE1, TIR1; Auxin/ INDOLE-3-ACETIC ACID INDUCIBLE, Aux/IAA; basic helix–loop–helix, bHLH; Malondialdehyde, MDA; abscisic acid, ABA

* Corresponding author. State Key Laboratory of Plant Physiology and Biochemistry, Institute of Genetics and Regenerative Biology, College of Life Sciences, Zhejiang University, Yuhangtang Road 866, Hangzhou, 310058, Zhejiang, China.

E-mail address: ninghan@zju.edu.cn (N. Han).

https://doi.org/10.1016/j.plaphy.2019.07.021
Received 21 June 2019; Received in revised form 17 July 2019; Accepted 21 July 2019
Available online 22 July 2019

Besides *ARF*-mediated auxin signal transduction, auxin perception is also regulated by miRNAs. miR393, which belongs to a conserved miRNA family discovered in many plants, targets genes encoding a small subset of F-box-containing auxin receptors, including TRANSPORT INHIBITOR RESPONSE1 (TIR1) and AFBs in *Arabidopsis* (Navarro et al., 2006), rice (Bian et al., 2012), and barley (Bai et al., 2017a). As components of the Skp1-Cullin1-F-box protein (SCF) ubiquitin ligase complexes, TIR1/AFBs release the activity of ARF transcription factors by presenting Auxin/Indole-3-Acetic Acid-inducible (Aux/IAA) repressors to proteolysis (Dharmasiri et al., 2005; Kepinski and Leyser, 2005). miR393 functions as an important regulator of auxin signaling (Iglesias et al., 2014; Windels et al., 2014), and affects various processes, including leaf, root development (Bian et al., 2012; Chen et al., 2011; Parry et al., 2009), the embryogenic transition induced in vitro (Wojcik and Gaj, 2016), and plant responses to biotic stress (Navarro et al., 2006; Robert-Seilaniantz et al., 2011). In addition, miR393 was reported to control root system architecture in response to nitrate availability, salinity stress in *Arabidopsis*, and inhibition of root elongation in response to toxic aluminum stress in barley (Bai et al., 2017a; Iglesias et al., 2014; Vidal et al., 2010). Together, these data demonstrate that the miR393/target module presents a conserved mechanism to regulate developmental processes and plant growth in response to environmental signals, through the auxin signaling pathway.

Stomata are openings in the epidermis of plant leaves with central roles in the exchange of water vapor and carbon dioxide between the plant and the environment. The development and patterning of stomata have emerged as an ideal system for studying position-dependent patterning via intercellular signaling, and the regulation of balance between proliferation and cell specification (Hepworth et al., 2018). On the other hand, the opening and closing of stomata, which are regulated by the integration of environmental signals and endogenous hormonal stimuli, affect the response and tolerance of plants towards drought stress conditions (Daszkowska-Golec and Szarejko, 2013). Recent publications identify the phytohormone auxin as a novel regulator of stomatal development and distribution (Balcerowicz et al., 2014; Balcerowicz and Hoecker, 2014). Our previous findings of miR393 accumulation in stomatal guard cells in rice (Guo et al., 2016) also suggests potential stomata-related functions for miR393. However, it is still unclear whether miR393 functions in the established signaling network during stomatal development and its response to drought stress.

In this study, we showed that miR393 affects the expression of stomatal development-related genes via the auxin signaling pathway in barley, and positively regulates stomatal density in leaves, which might then contribute to variation of drought stress tolerance.

2. Materials and methods

2.1. Plant materials and growth conditions

Barley (*Hordeum vulgare* L. 'Golden Promise'), including wildtype and all transgenic plants, was used in this study. Seeds of barley were surface-sterilized, rinsed, then placed on water-saturated filter papers in 9 cm culture dishes, and kept at 24 °C in the dark for 36 h. The germinating seeds were transferred to 12-cm-diameter plastic pots, 5 seedlings/pot, with a mixture of soil and vermiculite (3:1) (Sun Gro Horticulture Canada Ltd.) and kept well-watered with nutrient solution (Zeng et al., 2017) under a 24 °C, 16 h light/8 h dark photoperiod in a controlled climate chamber. For drought treatment, barley plants were grown in soil for one month, and water content was maintained in the soil (~78%) by the daily weighing of pots. The plants were then exposed to drought stress (without watering) for 22 days.

For hydroponics, germinated seeds were transferred to 16-cm-diameter plastic pots, 15 seedlings/pot, containing normal nutrient solution as described (Zeng et al., 2017). The nutrient solution was changed every 3 days. After 9 days' growth, the solution was renewed and the corresponding containers were supplemented with 20% (w/v) polyethylene glycol (PEG 6000) for simulated drought treatment. Each treatment contained at least 15 plants. For ABA treatment, germinated seeds were transferred to basic salt media (BSM) solution (0.5 mM KCl, 0.1 mM $CaCl_2$, pH 5.6) supplied with 50 μM ABA for an additional 24-h-growth. Each treatment contained at least 15 plants.

2.2. Vector construction and plant transformation

For the promoter:*GUS* constructs, an ~2 kb sequence upstream from the predicted fold-backs for miR393a and miR393b were amplified by PCR, and sub-cloned in pCAMBIA1301 to obtain *pMIR393a*:*GUS* and *pMIR393b*:*GUS*, respectively. The primers used in this work are listed in Supplemental Table S1. The clones used for vector construction were verified by sequencing. The constructs described were electroporated into *Agrobacterium tumefaciens* strain AGL1. The transformation was performed through the infection of immature embryos (IEs) -derived scutellum of barley with *Agrobacterium* followed by the selection of transgenic tissues on media containing 50 mg L^{-1} hygromycin (Harwood, 2014).

2.3. GUS staining

Histochemical localization of GUS staining was performed by incubating the seedlings in a solution of 1 mg mL^{-1} 5-bromo-4-chloro-3-indolyl-β-D-glucuronic acid (Sigma, USA), 1 mM potassium ferricyanide, 0.1% Triton X-100, 0.1 M sodium phosphate buffer, pH 7.0, and 10 mM EDTA at 37 °C, followed by clearing with 75% ethanol. Photos were taken with a Canon SLR camera.

2.4. RNA extraction and RT-PCR analysis

Total RNA from barley seedlings was extracted using RNAiso Plus (TaKaRa, Dalian, China), and 1 μg was used for first-strand cDNA synthesis using oligo (dT) primers and a Super-Script III RT kit (TaKaRa, Dalian, China). Quantitative real-time PCR (qRT-PCR) was performed on the Mastercycler Ep Realplex2 system (Eppendorf, Hamburg, Germany) using a SYBR PrimeScript RT reagent Kit (Perfect Real Time, TaKaRa, China). Relative transcript levels were calculated with the $^{\Delta\Delta}$Ct method and the *ACTIN* gene was used as a reference. Quantification of mature miRNA levels was carried out through a poly(A)-based real-time PCR approach using Mir-X™ miRNA First Strand Synthesis Kit (Clontech Laboratories, Inc., China, Cat. #638315). A preliminary test was performed using snoRNAs U6, miR168 and miR444 as internal controls for normalization mature miR393 level in qRT-PCR. The stability of reference gene expression was validated based on the standard deviation of the Ct value and coefficient of correlation. miR444 was found to be a suitable reference gene for its relative stable expression, and was used for normalization of miR393 level during seedling development and in ABA treatment experiment. Sequences of primers are listed in Table S1. The data shown were obtained from three biological replicates.

2.5. Microscopy-based analyses of stomata

For DIC imaging, a thin layer of nail varnish was applied on the lower epidermis in the region of maximum leaf width. After air drying, the varnished area was peeled off from the leaves using forceps. Stomatal counts were determined from nail varnish impressions on glass slides using a Nikon Eclipse 80i/90i Microscope (Nikon, Japan) with Nomarski optics. Typically, 10 abaxial fields per leaf from at least 10 individual plants were counted.

2.6. Detection of MDA and H_2O_2 accumulation

After drought treatment, 3, 3′-diaminobenzidine (DAB) staining of leaf samples was performed, as described previously (Bai et al., 2017a). The thiobarbituric acid (TBA) test, which determines MDA as an end product of lipid peroxidation, was used to measure lipid peroxidation in leaves. After

drought treatment, leaf material (1 g) was homogenized in 10 mL 10% (w/v) TCA solution. The homogenate was centrifuged at 5000 g for 10 min, and 2 mL of the supernatant was added to 2 mL 0.6% (w/v) TBA. The mixture was incubated in boiling water for 15 min, and the reaction was stopped by transferring the reaction tubes to an ice bath. The samples were then centrifuged at 5000 g for 5 min, and the absorbance of supernatant was read at 532, 600 and 450 nm. The content of MDA is calculated using the following formula: C ($\mu mol \cdot g^{-1}$ Fw) = 0.129 × (A_{532}-A_{600}) - 0.0112 × A_{450}. C represents the content of MDA. A_{532}, A_{600} and A_{450} refer to the absorbance values measured at three wavelengths, respectively. All spectrophotometric analyses were conducted at room temperature on a UV/visible spectrophotometer Hitachi U-3010 (Hitachi High-Technologies Corporation, Tokyo, Japan), and were repeated three times.

2.7. ABA content determination

1 g of two–week-old seedlings with or without treatment, were used. The measurement of ABA content was performed according to the product manual by using an enzyme-linked immunosorbent assay kit (Jiangsu Mei Biao Biological technology Co., Ltd, China, Cat. MB-3468A).

2.8. Statistical analysis

Values derived from three biological replicates were used to calculate standard deviations, and statistical significance was assessed using the Student's *t*-test and one-way ANOVA across genotypes for a given treatment at $p = 0.05$ or 0.01 with Tukey's posthoc test using OriginPro 8.5.1 (Origin Lab Corporation, Northampton, MA, USA). In graphs, values that differ significantly are indicated by asterisk (Figs. 1–7) or different letters (Figs. 6–7). Bars with similar or no letters indicate no statistical difference among genotypes under a given treatment.

3. Results

3.1. The spatial expression pattern of miR393 at different stages during development

In our previous work, we identified miR393 and its two target genes, *HvTIR1* and *HvAFB* in barley. Northern blot analysis showed that miR393 exhibited specific spatio-temporal expression pattern during seedling development (Bai et al., 2017a). In order to monitor the expression profile of miR393 in detail, two promoter-reporter lines, including *pMIR393a:GUS* and *pMIR393b:GUS*, were generated through *Agrobacterium tumefaciens*-mediated transformation of barley. In general, *pMIR393a* and *pMIR393b* displayed similar expression pattern during development (Fig. 1A and B; Fig. S1). In imbibed seeds, GUS staining was found in embryos, with a strong signal in the scutellum (Fig. 1C, Fig. S1A). After germination, GUS expression driven by the *MIR393* promoter was observed in the tip of coleoptiles, the shoot-root junction, and root (Fig. 1D–F and Figs. S1B–D). In leaves, the *MIR393a* promoter was active in the distal parts of the leaf blade, especially in guard cells (Fig. 1G, H and Figs. S1E and F). Furthermore, *pMIR393b:GUS* expression was detected in the stigma, style, anther and immature embryo (Figs. S1G–K) at the flowering stage. These data indicate that the expression of miR393 is active almost throughout the developmental period in barley. qRT-PCR detection of mature miRNA showed that the levels of miR393a and miR393b were increased with the seedling growth, and the abundance of miR393a was higher than that of miR393b in most of the tissues we tested. Both miR393a and miR393b were expressed preferentially in leaf and shoot, rather than in root (Fig. 1I).

3.2. miR393 affects leaf size and seedling growth in barley

To explore the biological function of miR393 in barley, we generated two transgenic barley lines. One was constructed to overexpress miR393 under a CaMV 35S promoter (*35S::MIR393b*; termed as *OE*), and the other was to inhibit miR393 activity through the target mimics strategy (*35S::MIM393,* termed as *MIM*. Besides root and seed phenotypes, which were reported in our previous papers (Bai et al., 2017a; Bai et al., 2017b), leaf size and shoot height of seedlings were altered in miR393 *OE* and *MIM* transgenic lines. As shown in Fig. 2A–B, the shoot lengths of *OE* and *MIM* transgenic lines were considerably lower after 14 days growth than those of the wild type (WT). Moreover, the *OE* line displayed adaxial rolled-leaf phenotype (Figs. S2A and B), and the leaf width was significantly lower than that of the WT (Fig. 2C and D). Both *OE* and *MIM* lines exhibited increased leaf angles (Fig. S2C), suggesting that miR393 is likely to regulate shoot architecture in barley.

3.3. miR393 regulates stomatal density and guard cell length in leaf blades

The expression of miR393 in guard cells prompted us to examine the stomata and guard cells in the transgenic plants. The first true leaves of 7-day-old seedlings were used for microscopic observations. Stomata in barley are characterized by dumbbell-shaped guard cells (GCs) flanked by subsidiary cells (SCs) and are always oriented in the same direction (Fig. 3). Overexpression of miR393 led to an increase in the abaxial stomatal density. In addition, the guard cell lengths in the *OE* line were significantly decreased. On the other hand, suppression of miR393 activity resulted in a phenotype opposite to that in the *OE* line, with decreased stomatal density and increased guard cell width (Fig. 3A–D). However, no significant change in stomatal lineage index (the ratio of stomata and arrested stomatal precursor cells to the total number of epidermal cells) was observed in both *OE* and *MIM* lines, compared with that of the WT (Fig. S3).

3.4. Expression levels of stomata development-related genes are altered in miR393 transgenic barley lines

In order to investigate the effect of miR393 on stomata development-related genes in barley, we searched for *EPIDERMAL PATTERNING FACTOR* (*EPF*), *SPCH*, *MUTE*, and *FAMA* orthologues in the barley genome and found four putative genes. We subsequently performed phylogenetic analysis of the proteins they encoded in *Arabidopsis*, rice and *Brachypodium distachyon* (Fig. 4A). According to sequence alignment, the protein sequence of HvSPCH shares 94% similarity to BdSPCH1, the latter is one of two functional but partially redundant SPCH paralogs in *Brachypodium* having arisen from a duplication event that occurred in grasses (Raissig et al., 2017). HvMUTE and HvFAMA can be grouped into the same clade with BdMUTE and BdFAMA, respectively. As for HvFAMA, it seems to evolve parallel to OsEPF and BdEPF.

The expression of stomatal development-related genes was examined through quantitative reverse transcription-PCR (qRT-PCR). Total RNA was isolated from the first leaves of 3-day-old and 7-day-old seedlings. When the first leaf started to stretch out of the envelope of coleoptile (3 d-old seedlings), the expression levels of *EPF1, SPCH,* and *MUTE* were suppressed in the *OE* line, and were elevated in the *MIM* line. The transcript level of *FAMA* was significantly higher in the *OE* line, and remained unchanged in 3-day-old *MIM* line (Fig. 4B). When the first leaf became fully expanded (7-d-old seedlings), only subtle changes were observed for the transcript levels of the four genes we detected (Fig. 4C). These data indicate that miR393 might affect cell divisions and cell fate transition during stomatal development.

3.5. miR393 affects stomatal development through the auxin signaling pathway

ARF5, *IAA12* and *IAA17* are three auxin signaling-related genes involved in stomatal development in *Arabidopsis* (Zhang et al., 2014). Barley *ARF5*, *IAA12* and *IAA17* candidates were identified by BLASTP in the barley database (http://webblast.ipk-gatersleben.de/barley/viroblast.php) using the protein sequences from *Arabidopsis* and rice

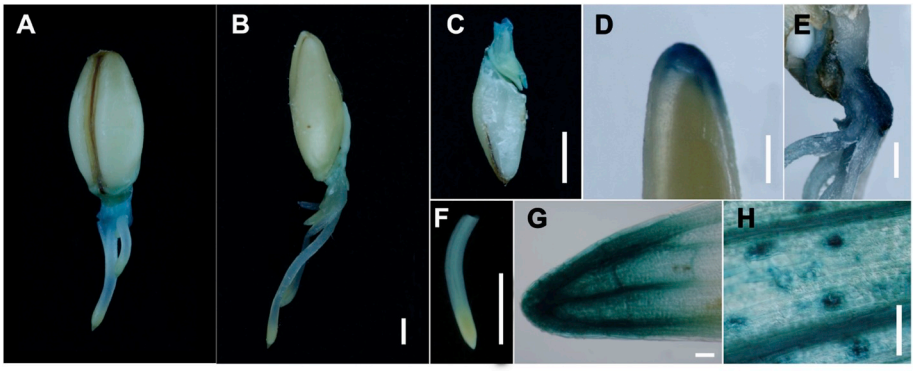

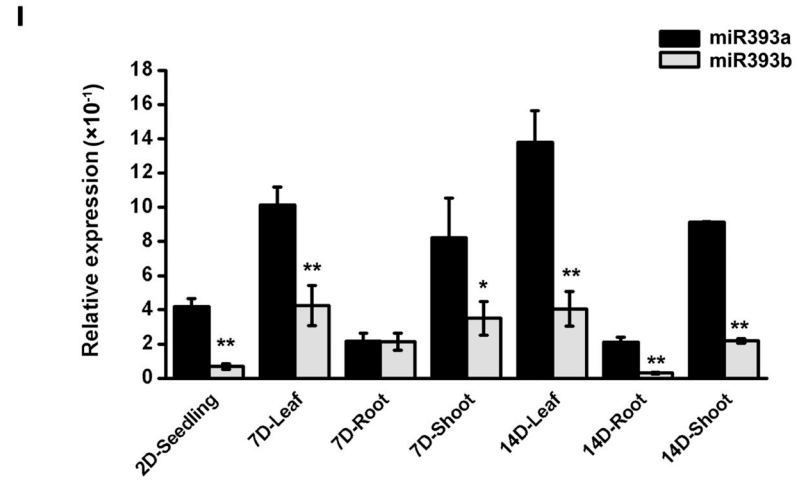

Fig. 1. Histochemical staining of *pMIR393a:GUS* and *pMIR393b:GUS* transgenic barley plants. (A) 1-d-old seedlings (1 day post germination) of *pMIR393a:GUS* (A) and *pMIR393b:GUS* (B). *pMIR393a* activity was detected in scutellum of the seed (C), coleoptile tip (D), the stem base (E) and root (F) of 1-d-old seedlings. GUS staining signals were found in the leaf (G), and stomatal guard cells of 14-day-old seedlings (H). A, B, C, G, scale bar = 2.5 mm; D, E, scale bar = 0.5 mm; H, J, scale bar = 0.1 mm. (I) qRT-PCR detection of miR393a and miR393b in wildtype barley at the vegetative growth stage. Total RNA was isolated from tissues in 2 d-, 7 d- and 14-d-old seedlings grown in the nutrient solution. The data shown are means ± S.D. from three biological replicates. Expression relative to miR444 are shown. Asterisks show significant difference between miR393a and miR393 b at the same tissue and growth stage (Student's *t*-test; $*p < 0.05$; $**p < 0.01$).

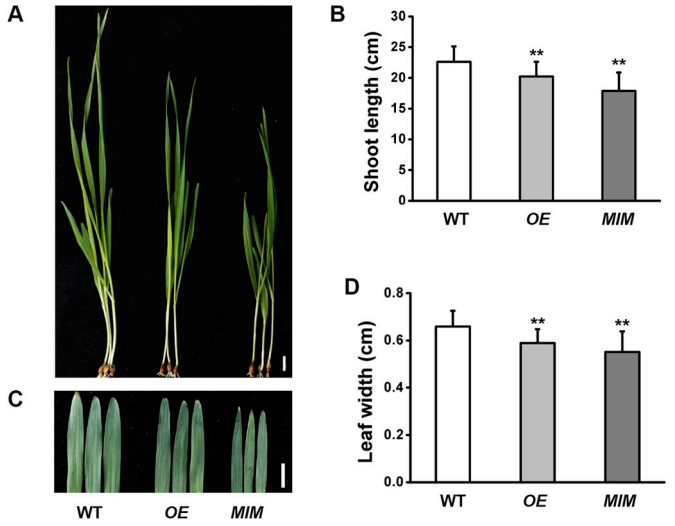

Fig. 2. miR393 regulates the leaf phenotype and shoot architecture of barley seedlings. A. Shoots of WT, *OE*, and *MIM* seedlings grown in the nutrient solution for 14 days. B. Quantification of shoot lengths. C. Leaf widths and leaf lengths of 14-day-old seedlings. Leaf phenotype of WT, *OE*, and *MIM* lines grown in the nutrient solution for 14 days. Scale bar = 1 cm. D. Quantification of leaf width. Error bars shown in Fig. 2B–D indicate S.D. for at least 30 plants. Asterisks show significant difference from WT (Student's *t*-test; $*p < 0.05$; $**p < 0.01$). The experiment was repeated three times with similar results.

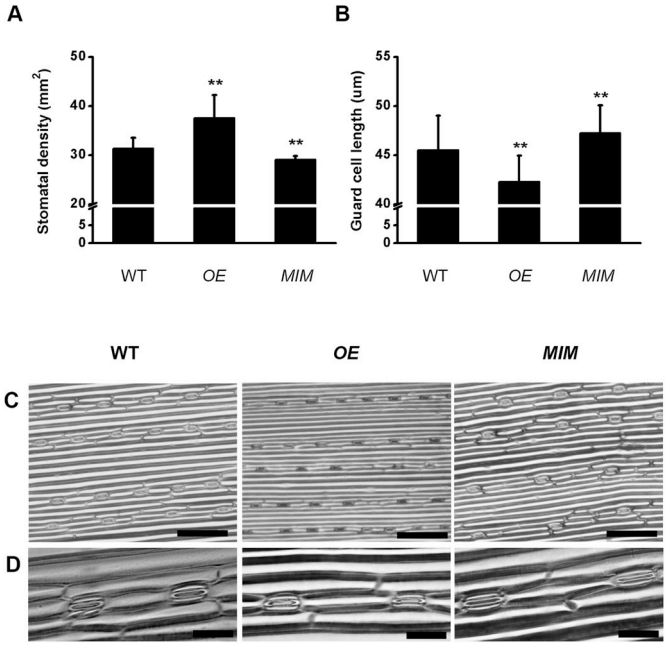

Fig. 3. Stomata phenotypes of WT, *OE*, and *MIM* lines. A. Abaxial stomatal density of WT, *OE*, and *MIM* lines. B. Stomatal guard cell lengths of WT, *OE*, and *MIM* lines. Three barley lines mentioned above were cultivated in the basic salt media (BSM) solution for 7 days. The data show means (± S.D) of 10 abaxial leaf fields from at least 10 individual plants for each genotype. Asterisks show significant difference from WT (Student's *t*-test; $*p < 0.05$; $**p < 0.01$). C-D. Abaxial epidermal micrographs of guard cells of WT, *OE*, and *MIM* transgenic lines. C, scale bar = 200 μm; D, scale bar = 50 μm.

as queries. We measured the expression of putative auxin-responsive genes in WT, *OE*, and *MIM* lines. Amongst them, *IAA12* and *IAA17* were up-regulated in both *OE* and *MIM* lines (Fig. 5A and Fig. S4). Only *ARF5* exhibited an opposite trend in *OE* and *MIM* lines in the leaves of 3 d-old

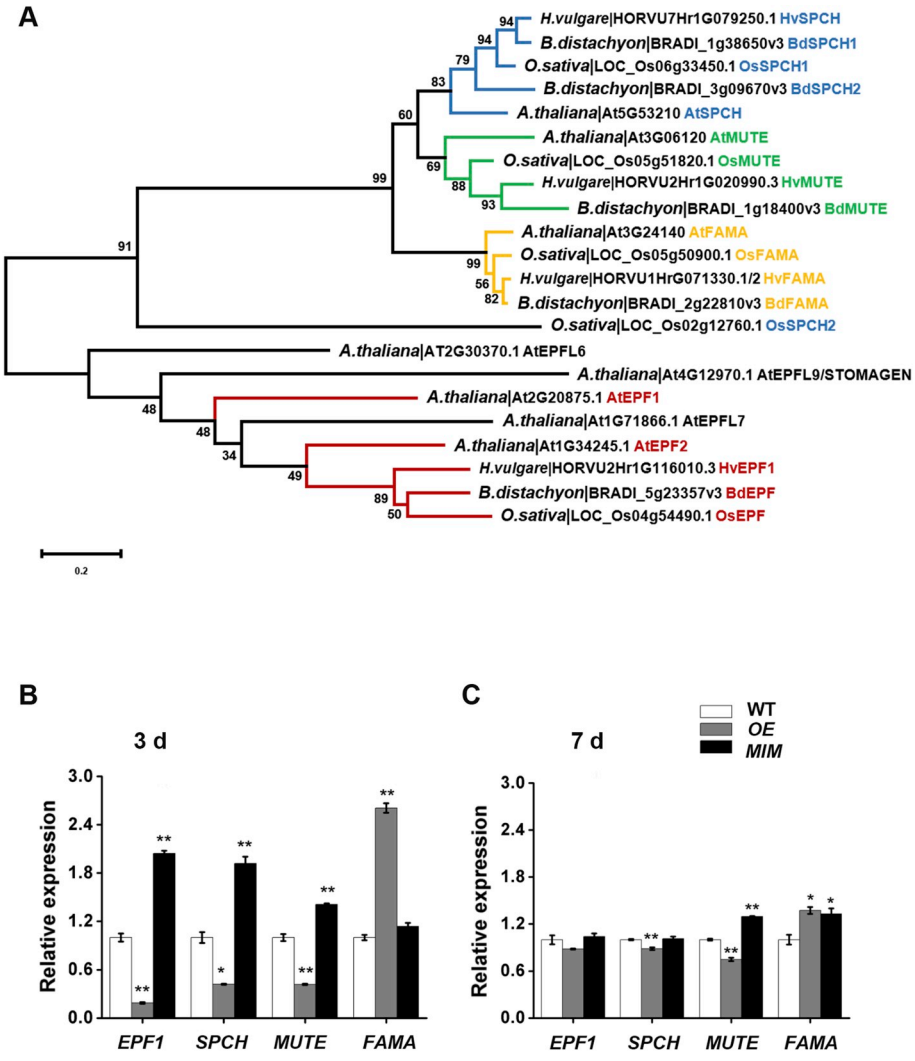

Fig. 4. miR393 influences the expression of stomatal development-related genes. *EPF1* (epidermal patterning factor 1), *SPCH* (SPEECHLESS), *MUTE*, and *FAMA* encode bHLH transcription factors associated with stomatal development. A. Phylogenetic tree of EPF1, SPCH, MUTE, and FAMA among barley and other species constructed in MEGA 4 by the Neighbor-Joining method. The gene IDs are *HvSPCH* (HORVU7Hr1G079250.1), *HvMUTE* (HORVU2Hr1G020990.3), *HvFAMA* (HORVU1HrG071330.1&2), and *HvEPF1* (HORVU2Hr1G116010.3) from *Hordeum vulgare*, from *Hordeum vulgare*, *BdSPCH1* (BRADI_1g38650v3), *BdSPCH2* (BRADI_3g08210v3), *BdMUTE* (BRADI_1g18400v3), *BdFAMA* (BRADI_2g22810v3), and *BdEPF* (BRADI_5g23357v3) from *Brachypodium distachyon*, *OsSPCH1* (LOC_Os06g33450.1), *OsSPCH2* (LOC_Os02g12760.1), *OsMUTE* (LOC_Os05g51820.1), *OsFAMA* (LOC_Os05g50900.1), and *OsEPF* (LOC_Os04g54490.1) from *Oryza sativa*, and *AtSPCH* (AT5G53210), *AtMUTE* (AT3G06120), *AtFAMA* (AT3G24140), *AtEPF1* (AT2G20875.1), *AtEPF2* (AT1G34245.1), and *AtEPFL9/STOMAGEN* (AT4G12970.1) from *Arabidopsis thaliana*. B–C. The expression of stomatal development-related genes. Total RNA was isolated from the first leaf of 3-day-old (B) and 7-day-old (C) seedlings grown in the BSM solution. The expression levels in WT were set as 1.0. The data shown are means ± S.D. of three biological replicates. Asterisks show significant difference from WT (Student's *t*-test; $*p < 0.05$; $**p < 0.01$).

seedlings. Overexpression of miR393 resulted in a significant decrease in *ARF5* transcript levels, while inhibiting miR393 activity led to a moderate increase in *ARF5* expression (Fig. 5A). When the first leaf became fully expanded (in 7-d-old seedlings), the transcript level of *ARF5* was decreased both in the *OE* and *MIM* lines (Fig. S4). The putative *HvARF5* (HORVU2Hr1G109650) encodes a protein of 955 amino acids. Using the Conserved Domain database (https://www.ncbi.nlm.nih.gov/cdd), three domains including B3 DNA binding domain, Auxin_resp (a conserved region of auxin-responsive transcription factors) and Aux_IAA super family, have been found for this predicted HvARF5 (Fig. 5B). The sequences of these domains are highly conserved among *Arabidopsis*, rice and barley (Fig. 5C).

3.6. Overexpression of miR393 enhanced drought sensitivity in barley

Next, we detected drought tolerance of WT, *OE*, and *MIM* plants. 30-day-old plants grown at 24 °C in a growth chamber were subjected to a terminal drought experiment, alongside a parallel set of plants that were kept well-watered. After 22 days drought treatment, an attenuated growth rate was observed in all three lines. Furthermore, the *OE* plants exhibited serious signs of wilting (Fig. 6A). MDA (malondialdehyde) content in leaves was measured to assess lipid peroxidation under drought treatment. As shown in Fig. 6B, drought treatment resulted in MDA accumulation in all three lines. The highest level of MDA occurred in the *OE* lines, suggesting that drought-induced lipid peroxidation was more severe in the *OE* line than in WT. As for the *MIM* line, water stress-induced oxidative damage in leaves was greatly alleviated compared to that in the WT.

The accumulation of reactive oxygen species (ROS) under drought stress is a common phenomenon which can cause oxidative damage in plant cells. The leaves of seedlings were stained with DAB, which can be used to visualize the production of H_2O_2. No DAB staining was observed in barley leaves under control treatment. After drought treatment, DAB staining became stronger in the leaves of the *OE* line, while no obvious change was observed in WT and the *MIM* line (Fig. 6C). Quantification of water loss rates in detached leaves indicated that the *MIM* line had slower rates of water evaporation than did the WT and the *OE* line (Fig. 6D). Together, these data suggested that miR393 might influence drought tolerance in barley.

3.7. miR393 might regulate drought tolerance through the ABA pathway

Abscisic acid (ABA) is a key phytohormone promoting abiotic stress tolerance, as well as developmental processes such as seed dormancy and germination. Water stress triggers a series of adjustments to plant physiology, including ABA biosynthesis and stomatal closure, to limit evapotranspiration (Kuromori et al., 2018). It was found that both the transcription of *pri-MIR393* and the accumulation of mature miR393 were induced under exogenous ABA treatment, especially for *pri-MIR393b* and miR393b (Fig. 7A and B). Moreover, miR393 transgenic lines exhibited differential ABA sensitivity. Overexpression of miR393 led to increased ABA sensitivity, whereas knocking down miR393

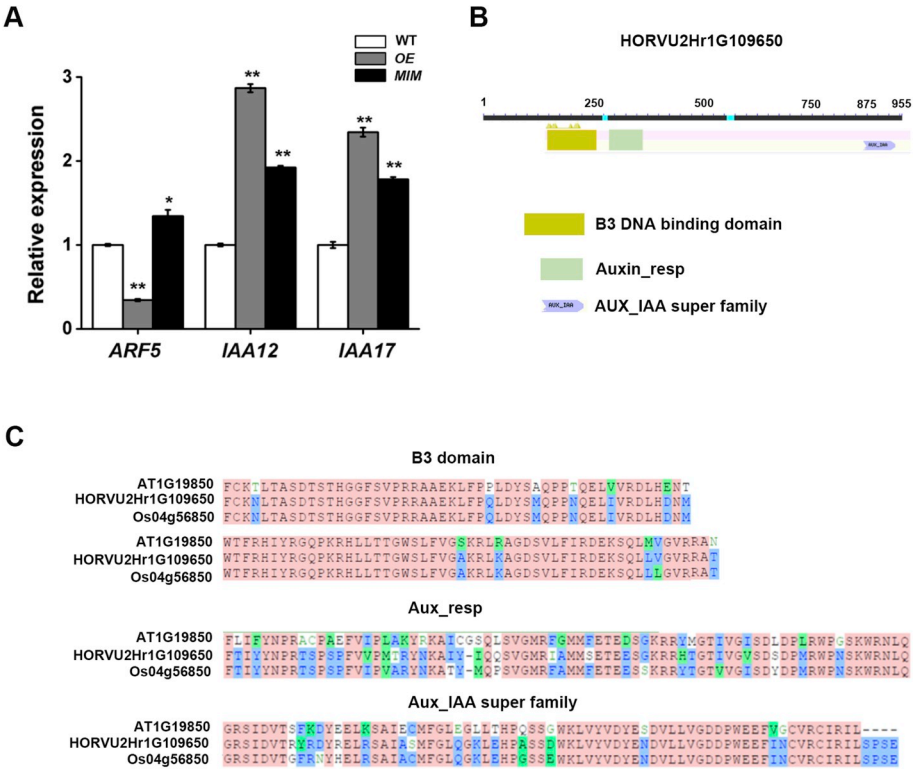

Fig. 5. miR393 affects the expression of auxin-responsive genes during barley stomatal development. A. The expression of auxin-responsive genes. Total RNA was isolated from the first leaf of 3-day-old seedlings grown in the BSM solution. The expression level of corresponding genes in WT were set as 1.0. The data shown are means ± S.D. of three biological replicates. Asterisks show significant differences from WT (Student's *t*-test; $*p < 0.05$; $**p < 0.01$). B. The structure of a putative ARF5 in barley. The structure of protein encoded by HORVU2Hr1G109650 was predicted through the Conserved Domain database (https://www.ncbi.nlm.nih.gov/cdd). C. Sequence alignment of three ARF5 homologs from *Arabidopsis*, rice and barley. Only the sequences of B3 DNA binding domain, Auxin_resp (a conserved region of auxin-responsive transcription factors) and Aux_IAA super family are shown. The gene IDs are HORVU2Hr1G109650 from *Hordeum vulgare*, LOC_Os04g56850.1 from *Oryza sativa*, and AT1G19850.1 from *Arabidopsis thaliana*.

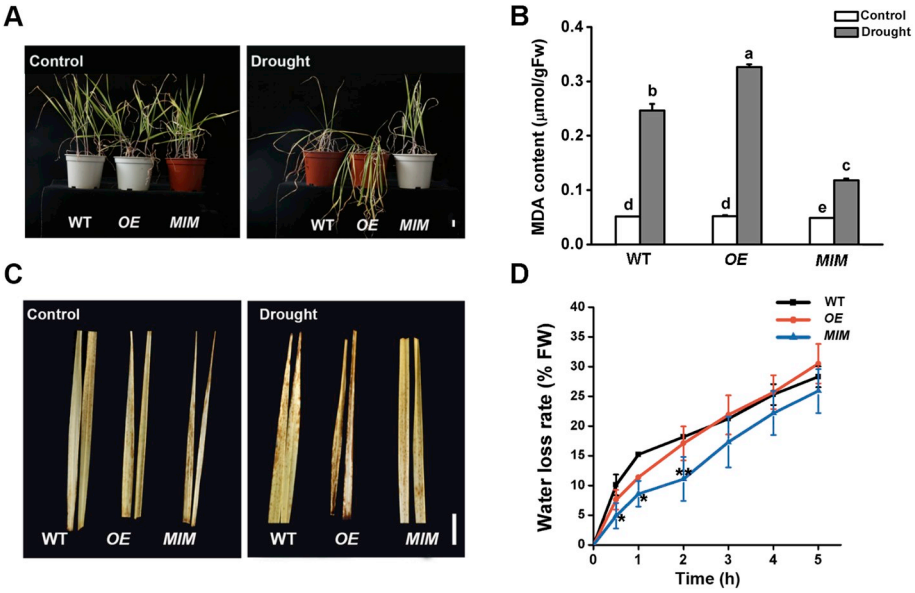

Fig. 6. Phenotypes of WT, *OE*, and *MIM* transgenic barley lines under drought treatment. A. Photographs of WT, *OE*, and *MIM* plants after drought treatment for 22 days. B. MDA (malondialdehyde) content in leaves of WT, *OE*, and *MIM* lines after 22 days drought treatment. The data shown are means ± S.D., n = 15 seedlings, three replicates. Values that differ significantly are indicated by different letters (Student's *t*-test; $*p < 0.05$; $**p < 0.01$). C. DAB (3, 3′-Diaminobenzidine) staining of untreated and drought-stressed leaves in WT, *OE*, and *MIM* lines. D. Rate of relative water loss of detached leaves. The leaf samples (about 1 g) were detached from the same stage of different plants growing under normal conditions for four weeks, weighed immediately on a piece of weighing paper, and then placed on a laboratory bench and weighed at designated times. The percentage loss of fresh weight was calculated on the basis of the initial weight of the plants. The data shown are means ± S.D., n = 15, three replicates. Asterisks show significant difference from WT under a given treatment (Student's *t*-test; $*p < 0.05$; $**p < 0.01$). A, scale bar = 2 cm; C, scale bar = 1 cm.

activity reduced ABA sensitivity, as reflected in the seed germination and leaf greening rates under ABA treatment (Figs. S5A and B). These data suggested that miR393 not only regulates auxin signaling, but also interacts with the ABA pathway.

In order to investigate whether the alteration of miR393 levels affects ABA biosynthesis under water limiting conditions, we tested ABA-related gene expression and ABA content in leaves. Our results showed that 20% PEG treatment considerably induced the expression of ABA biosynthesis-related genes (*NCED1*, *NCED2* and *NCED3*), indicating that water stress promoted ABA production (Fig. 7C). Moreover, ABA content exhibited a significant difference among three lines. PEG-induced ABA synthesis was inhibited, especially in the miR393-overexpressing line. The *MIM* line displayed significantly increased ABA levels both under normal or water-deficient conditions, compared with their WT controls (Fig. 7D). These data provided a possibility that miR393 might regulate drought response and tolerance through its crosstalk with the ABA pathway.

4. Discussion

In barley, the miRNA393 family consists of two members: miR393a and miR393b, which are encoded by *HvMIR393a* and *HvMIR393b*, respectively. Mature miR393a and miR393b differ in sequence by a 1-nt downstream shift in the annotated start sites (Bai et al., 2017a). A

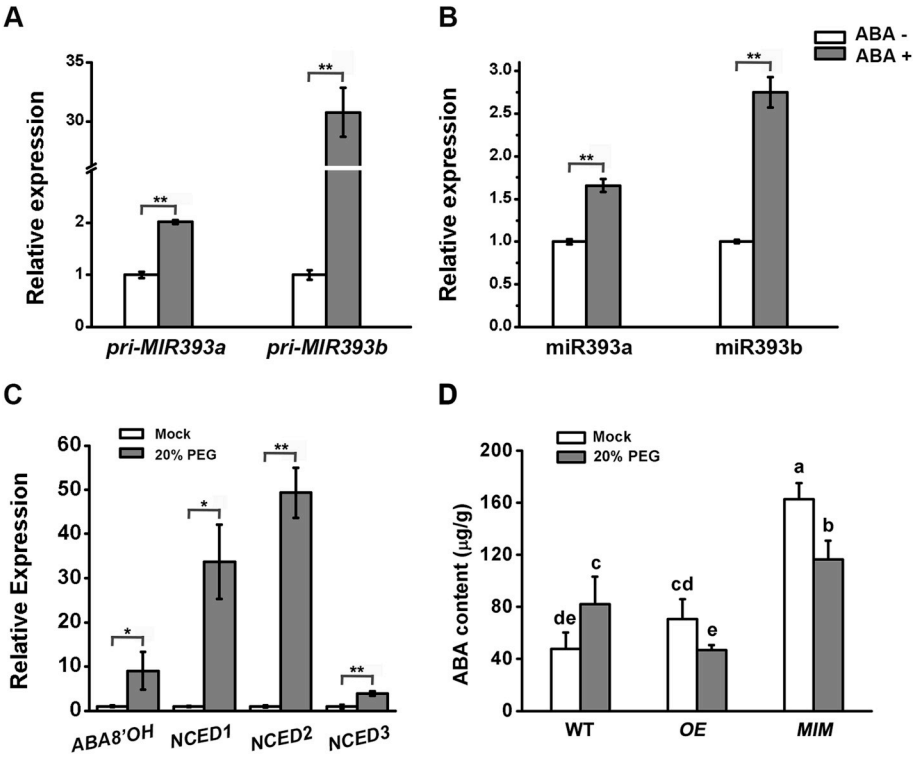

Fig. 7. miR393 might regulate drought tolerance through the ABA pathway. A-B. The expression of *pri-MIR393* (A) and mature miR393 (B) in response to exogenous ABA treatment. The germinated wild type seeds (n = 15) were grown in the BSM solution containing 0 or 50 μM ABA for 24 h. Total RNA was isolated from leaf tissues. The data shown are means ± S.D. of three biological replicates. Asterisks show significant difference from mock (ABA-) treatment (Student's *t*-test; $*p < 0.05$; $**p < 0.01$). C. The expression of ABA-related genes *ABA 8'OH*, *NCED1*, *NCED2*, and *NCED3* in response to PEG treatment. 9-day-old seedlings (n = 15) were exposed to 20% PEG treatment. The data shown are means ± S.D. of three biological replicates. Asterisks show significant difference from mock treatment (Student's *t*-test; $*p < 0.05$; $**p < 0.01$). D. ABA content in leaf tissues of WT, *OE*, and *MIM* lines after 20% PEG treatment for 24 h. The data shown are means ± S.D., n = 15, three replicates. Values that differ significantly are indicated by different letters (Student's *t*-test; $*p < 0.05$; $**p < 0.01$).

combination of promoter reporter analysis and RT-PCR detection have been performed to reveal the expression pattern of different miR393 members. Although the sequences of the two promoters are almost completely different, they contain several common conservative cia-acting regulatory elements, such as elements essential for light induction, anaerobic induction, and elements involved in drought-inducibility and low-temperature responsiveness (Fig. S6). Histochemical detection of GUS activity showed that *MIR393a* and *MIR393b* displayed similar spatial expression patterns, both were transcribed in germinated seed, roots and leaves (Fig. 1 and Fig. S1). The results of qRT-PCR detection of mature miR393 were consistent with previous RNA gel blot data (Bai et al., 2017a), indicating that the level of miR393 was higher in aerial tissues than in the underground organs. It was also found that the relative level of miR393a is higher than miR393b (Fig. 1I), suggesting that *MIR393a* seems to contribute more to the accumulation of mature miR393 during early seedling growth stages.

The biological function of miR393 was investigated using miR393 overexpression and target mimic transgenic barley lines. Leaf size and shoot height of seedlings was found to be decreased significantly in miR393 *OE* and *MIM* transgenic lines after 14-day-growth (Fig. 2). Because the conserved targets of miR393 belong to the TIR1/AFBs family of auxin receptors, we proposed that ectopic expression of miR393 or inhibition of miR393 activity might disrupt auxin homeostasis, which might be required for normal seedling growth in barley.

The following work focuses on stomata. The formation and distribution of stomata is tightly regulated by intrinsic and environmental signals, thereby representing an excellent system to study the fundamental mechanisms that control cell fate and patterning (Qi and Torii, 2018). In the study herein, we showed that miR393, which regulates auxin *TIR1/AFBs* co-receptor genes post-transcriptionally, is involved in stomatal development in barley. Using a promoter-reporter line, *MIR393* expression could be detected in the stomata of young leaves (Fig. 1H and 1SF). Similar results have been reported in rice (Guo et al., 2016). Observations in *Arabidopsis* by analyzing DR5 and DII-Venus auxin output and input reporters respectively, provided further evidence for auxin signaling during stomatal development (Le et al., 2014). These data indicated that miR393 might be helpful for precise regulation of auxin signaling for determination of cell fate and cell division during stomatal development.

Transgenic barley plants, including miR393 overexpressing or knock-down lines, were used to unravel the function of miR393 in stomatal development. It showed that overexpression of miR393 resulted in increased stomatal density, whereas knocking down miR393 activity caused an opposite phenotype. This is in agreement with the phenotype of a quadruple mutant *tir1 afb1 afb2 afb3* in *Arabidopsis*, which displayed prominent stomatal clusters and increased SMI (the proportion of stomata among all epidermal cells), indicating that nuclear receptor-mediated auxin signaling is required for negative regulation of stomatal development (Zhang et al., 2014). Considering the intermediate stomatal phenotype observed in the *OE* line, we proposed that, besides miR393 target genes, other components in auxin pathway might be involved in the regulation of stomatal development in barley.

qRT-PCR detection of auxin-related genes allowed the identification of a candidate gene which could be involved in auxin responses during stomatal development. The results showed that the transcript level of putative *ARF5* (also known as MONOPTEROS, MP) decreased in the *OE* line, and was enhanced in the *MIM* line, indicating a negative relationship with miR393 (Fig. 5A). In *Arabidopsis*, significantly increased SMI and stomatal clusters have been reported in the lethal *mp* allele in *arf5-1* seedlings. Furthermore, through physiological, genetic, biochemical, and molecular analyses, MP was found to repress the expression of STOMAGEN by directly binding to its promoter (Zhang et al., 2014). We further detected the expression of a putative STOMAGEN gene (HORVU3Hr1G093110.9) in barley. The protein sequence of this candidate shares 47.8% similarity to the STOMAGEN from Arabidopsis, and is predicted as an EPIDERMAL PATTERNING FACTOR-like protein (Fig. S7A). qRT-PCR showed that, in the 7-day-old seedlings, the transcript level of this STOMAGEN putative gene in the first leaf was elevated significantly in the *OE* line, and was repressed in the *MIM* line (Fig. S6C). These data raise a possibility that *ARF5* might act as a downstream factor linking auxin response to stomatal development in barley, although further experiments are needed to validate its biological function and elucidate related mechanisms. On the other hand, two AUX/IAA genes, *IAA12* and *IAA17*, were found to be up-

regulated in both the *OE* and the *MIM* lines (Fig. 5A, Fig. S4). It indicates that the transcript levels of *IAA12* and *IAA17* might not be regulated directly by miR393 or its targets. According to the current auxin signaling model, the target genes *TIR1/AFBs*, which encoding auxin co-receptors, regulate auxin signaling by proteolysis of Aux/IAA repressors (Dharmasiri et al., 2005; Kepinski and Leyser, 2005). Whether miR393 regulates the protein stability of IAA12 and IAA17 need to be further studied.

To explain how miR393 affects stomatal development, we monitored the expression of four transcription factors in the transgenic lines. Our results showed that miR393 plays a role in gene regulation mainly in early stages of leaf development, and the expression of three genes (*EPF1*, *SPCH*, and *MUTE*) was suppressed in the *OE* line, but was enhanced in the *MIM* line (Fig. 4B). These observations are of particular interest when considering the grasses, because both the morphology of guard cells and their tissue distributions differ substantially from *Arabidopsis*. Except FAMA, whose function is conserved between monocots and dicots, the roles of MUTE and two SPCH paralogs are divergent (Liu et al., 2009). Studies in *Brachypodium* demonstrate that the expression of *BdSPCH1* and *BdSPCH2* is limited to the stomatal cell file during stomatal development (Raissig et al., 2016), while *BdMUTE* moves from guard mother cells (GMCs) into neighboring subsidiary mother cells (SMCs) to establish SMCs identity (Raissig et al., 2017). *HvEPF1*, a barley orthologue of *AtEPF1/2*, is found to prevent GMC formation and cause the arrest of GMC development prior to SMC generation (Hughes et al., 2017). Therefore, we proposed that the regulation of miR393 might be associated with asymmetric division in the early stages of stomatal development, especially for subsidiary cell formation (Hepworth et al., 2018). Research in *Z. mays* supports our speculation and provides evidence that auxin is involved in subsidiary cell formation, probably functioning as an inducer of asymmetric SMC division (Livanos et al., 2015).

The majority of water loss from plants occurs via transpiration through stomata, making these cellular structures an attractive target for improving drought tolerance. Since miR393 affects stomatal density and guard cell length, we were interested in investigating whether it regulates water loss and drought tolerance. After 22 days drought treatment, the *MIM* line exhibited enhanced drought tolerance, as reflected by alleviated leaf wilting and MDA accumulation, compared with WT, whereas the *OE* line became more sensitive to water-limiting treatment (Fig. 6). A previous study in barley showed that overexpression of *HvEPF1*, a gene which belongs to the epidermal patterning factor (EPF) family of secreted signaling peptides, resulted in significantly reduced stomatal density, substantial reductions in leaf gas exchange, remarkably enhanced water use efficiency, and drought tolerance. In addition, *HvEPF1OE* barley lines showed no reductions in grain yield (Hughes et al., 2017). Therefore, alterations in stomatal density might contribute to drought tolerance in barley.

Besides stomatal density, stomatal aperture is another factor that might affect water loss. In response to drought, plants synthesize the hormone ABA, which triggers stomatal closure, thus reducing transpirational water loss. ABA-induced stomatal closure has been observed in many plant species including barley (Shen et al., 2015). We found that miR393 altered ABA biosynthesis-related genes 9-cis-epoxycarotenoid dioxygenase (*NCED1*, *NCED2*, and *NCED3*; Fig. 7C), which is consistent with the ABA levels among the three lines (Fig. 7D). Moreover, we found that miR393 is an ABA-responsive miRNA; the expression of both miR393a and miR393b was induced in leaf samples of barley seedlings when exogenous ABA was applied (Fig. 7A, B), and plant sensitivity to ABA treatment was altered in transgenic miR393 lines (Fig. S5). Thus we propose that miR393 might regulate drought tolerance via ABA-induced stomatal closure or other cellular responses that protect cells from desiccation damage.

Collectively, we found that miR393 positively regulates the stomatal density in leaves, and controls ABA accumulation under drought stress. Understanding these control systems will help us to develop plant varieties that are better able to withstand drought conditions.

Contributions

Muyuan Zhu and Ning Han designed the research, Weiyi Yuan, Bo Shi, Jingqi Suo and Bin Bai performed the experiments, and Weiyi Yuan, Bo Shi and Chenlu Zhou analyzed the data, Ning Han and Hongwu Bian wrote the paper.

Acknowledgements

This work was supported by the National Natural Science Foundation of China [31571645], the earmarked fund for China Agricultural Research System (CARS-05-05A) and the Science Foundation of Zhejiang Province [LGN18C130001].

Appendix A. Supplementary data

Supplementary data to this article can be found online at https://doi.org/10.1016/j.plaphy.2019.07.021.

References

Bai, B., Bian, H., Zeng, Z., Hou, N., Shi, B., Wang, J., Zhu, M., Han, N., 2017a. miR393-Mediated auxin signaling regulation is involved in root elongation inhibition in response to toxic aluminum stress in barley. Plant Cell Physiol. 58, 426–439.
Bai, B., Shi, B., Hou, N., Cao, Y., Meng, Y., Bian, H., Zhu, M., Han, N., 2017b. microRNAs participate in gene expression regulation and phytohormone cross-talk in barley embryo during seed development and germination. BMC Plant Biol. 17, 150.
Balcerowicz, M., Hoecker, U., 2014. Auxin–a novel regulator of stomata differentiation. Trends Plant Sci. 19, 747–749.
Balcerowicz, M., Ranjan, A., Rupprecht, L., Fiene, G., Hoecker, U., 2014. Auxin represses stomatal development in dark-grown seedlings via Aux/IAA proteins. Development 141, 3165–3176.
Bian, H., Xie, Y., Guo, F., Han, N., Ma, S., Zeng, Z., Wang, J., Yang, Y., Zhu, M., 2012. Distinctive expression patterns and roles of the miRNA393/TIR1 homolog module in regulating flag leaf inclination and primary and crown root growth in rice (Oryza sativa). New Phytol. 196, 149–161.
Cabrera, J., Barcala, M., Garcia, A., Rio-Machin, A., Medina, C., Jaubert-Possamai, S., Favery, B., Maizel, A., Ruiz-Ferrer, V., Fenoll, C., Escobar, C., 2016. Differentially expressed small RNAs in Arabidopsis galls formed by Meloidogyne javanica: a functional role for miR390 and its TAS3-derived tasiRNAs. New Phytol. 209, 1625–1640.
Chen, Z.H., Bao, M.L., Sun, Y.Z., Yang, Y.J., Xu, X.H., Wang, J.H., Han, N., Bian, H.W., Zhu, M.Y., 2011. Regulation of auxin response by miR393-targeted transport inhibitor response protein 1 is involved in normal development in Arabidopsis. Plant Mol. Biol. 77, 619–629.
Daszkowska-Golec, A., Szarejko, I., 2013. Open or close the gate - stomata action under the control of phytohormones in drought stress conditions. Front. Plant Sci. 4, 138.
Dharmasiri, N., Dharmasiri, S., Estelle, M., 2005. The F-box protein TIR1 is an auxin receptor. Nature 435, 441–445.
Guo, F., Han, N., Xie, Y., Fang, K., Yang, Y., Zhu, M., Wang, J., Bian, H., 2016. The miR393a/target module regulates seed germination and seedling establishment under submergence in rice (Oryza sativa L.). Plant Cell Environ. 39, 2288–2302.
Harwood, W.A., 2014. A protocol for high-throughput Agrobacterium-mediated barley transformation. Methods Mol. Biol. 1099, 251–260.
Hepworth, C., Caine, R.S., Harrison, E.L., Sloan, J., Gray, J.E., 2018. Stomatal development: focusing on the grasses. Curr. Opin. Plant Biol. 41, 1–7.
Hobecker, K.V., Reynoso, M.A., Bustos-Sanmamed, P., Wen, J., Mysore, K.S., Crespi, M., Blanco, F.A., Zanetti, M.E., 2017. The MicroRNA390/TAS3 pathway mediates symbiotic nodulation and lateral root growth. Plant Physiol. 174, 2469–2486.
Hughes, J., Hepworth, C., Dutton, C., Dunn, J.A., Hunt, L., Stephens, J., Waugh, R., Cameron, D.D., Gray, J.E., 2017. Reducing stomatal density in barley improves drought tolerance without impacting on yield. Plant Physiol. 174, 776–787.
Iglesias, M.J., Terrile, M.C., Windels, D., Lombardo, M.C., Bartoli, C.G., Vazquez, F., Estelle, M., Casalongue, C.A., 2014. MiR393 regulation of auxin signaling and redox-related components during acclimation to salinity in Arabidopsis. PLoS One 9, e107678.
Kepinski, S., Leyser, O., 2005. The Arabidopsis F-box protein TIR1 is an auxin receptor. Nature 435, 446–451.
Kieffer, M., Neve, J., Kepinski, S., 2010. Defining auxin response contexts in plant development. Curr. Opin. Plant Biol. 13, 12–20.
Kuromori, T., Seo, M., Shinozaki, K., 2018. ABA transport and plant water stress responses. Trends Plant Sci. 23, 513–522.
Le, J., Liu, X.G., Yang, K.Z., Chen, X.L., Zou, J.J., Wang, H.Z., Wang, M., Vanneste, S., Morita, M., Tasaka, M., Ding, Z.J., Friml, J., Beeckman, T., Sack, F., 2014. Auxin transport and activity regulate stomatal patterning and development. Nat. Commun. 5, 3090.
Liu, P.P., Montgomery, T.A., Fahlgren, N., Kasschau, K.D., Nonogaki, H., Carrington, J.C.,

2007. Repression of AUXIN RESPONSE FACTOR10 by microRNA160 is critical for seed germination and post-germination stages. Plant J. 52, 133–146.
Liu, T., Ohashi-Ito, K., Bergmann, D.C., 2009. Orthologs of Arabidopsis thaliana stomatal bHLH genes and regulation of stomatal development in grasses. Development 136, 2265–2276.
Livanos, P., Giannoutsou, E., Apostolakos, P., Galatis, B., 2015. Auxin as an inducer of asymmetrical division generating the subsidiary cells in stomatal complexes of Zea mays. Plant Signal. Behav. 10, e984531.
Marin, E., Jouannet, V., Herz, A., Lokerse, A.S., Weijers, D., Vaucheret, H., Nussaume, L., Crespi, M.D., Maizel, A., 2010. miR390, Arabidopsis TAS3 tasiRNAs, and their AUXIN RESPONSE FACTOR targets define an autoregulatory network quantitatively regulating lateral root growth. Plant Cell 22, 1104–1117.
Navarro, L., Dunoyer, P., Jay, F., Arnold, B., Dharmasiri, N., Estelle, M., Voinnet, O., Jones, J.D., 2006. A plant miRNA contributes to antibacterial resistance by repressing auxin signaling. Science 312, 436–439.
Nizampatnam, N.R., Schreier, S.J., Damodaran, S., Adhikari, S., Subramanian, S., 2015. microRNA160 dictates stage-specific auxin and cytokinin sensitivities and directs soybean nodule development. Plant J. 84, 140–153.
Parry, G., Calderon-Villalobos, L.I., Prigge, M., Peret, B., Dharmasiri, S., Itoh, H., Lechner, E., Gray, W.M., Bennett, M., Estelle, M., 2009. Complex regulation of the TIR1/AFB family of auxin receptors. Proc. Natl. Acad. Sci. U. S. A. 106, 22540–22545.
Qi, X., Torii, K.U., 2018. Hormonal and environmental signals guiding stomatal development. BMC Biol. 16, 21.
Raissig, M.T., Abrash, E., Bettadapur, A., Vogel, J.P., Bergmann, D.C., 2016. Grasses use an alternatively wired bHLH transcription factor network to establish stomatal identity. Proc. Natl. Acad. Sci. U.S.A. 113, 8326–8331.
Raissig, M.T., Matos, J.L., Anleu Gil, M.X., Kornfeld, A., Bettadapur, A., Abrash, E., Allison, H.R., Badgley, G., Vogel, J.P., Berry, J.A., Bergmann, D.C., 2017. Mobile MUTE specifies subsidiary cells to build physiologically improved grass stomata. Science 355, 1215–1218.
Robert-Seilaniantz, A., MacLean, D., Jikumaru, Y., Hill, L., Yamaguchi, S., Kamiya, Y., Jones, J.D., 2011. The microRNA miR393 re-directs secondary metabolite biosynthesis away from camalexin and towards glucosinolates. Plant J. 67, 218–231.
Shen, L., Sun, P., Bonnell, V.C., Edwards, K.J., Hetherington, A.M., McAinsh, M.R., Roberts, M.R., 2015. Measuring stress signaling responses of stomata in isolated epidermis of graminaceous species. Front. Plant Sci. 6, 533.
Vidal, E.A., Araus, V., Lu, C., Parry, G., Green, P.J., Coruzzi, G.M., Gutierrez, R.A., 2010. Nitrate-responsive miR393/AFB3 regulatory module controls root system architecture in Arabidopsis thaliana. Proc. Natl. Acad. Sci. U.S.A. 107, 4477–4482.
Voinnet, O., 2009. Origin, biogenesis, and activity of plant microRNAs. Cell 136, 669–687.
Wang, Y., Li, K., Chen, L., Zou, Y., Liu, H., Tian, Y., Li, D., Wang, R., Zhao, F., Ferguson, B.J., Gresshoff, P.M., Li, X., 2015. MicroRNA167-Directed regulation of the auxin response factors GmARF8a and GmARF8b is required for soybean nodulation and lateral root development. Plant Physiol. 168, 984–999.
Williams, L., Carles, C.C., Osmont, K.S., Fletcher, J.C., 2005. A database analysis method identifies an endogenous trans-acting short-interfering RNA that targets the Arabidopsis ARF2, ARF3, and ARF4 genes. Proc. Natl. Acad. Sci. U.S.A. 102, 9703–9708.
Windels, D., Bielewicz, D., Ebneter, M., Jarmolowski, A., Szweykowska-Kulinska, Z., Vazquez, F., 2014. miR393 is required for production of proper auxin signalling outputs. PLoS One 9, e95972.
Wojcik, A.M., Gaj, M.D., 2016. miR393 contributes to the embryogenic transition induced in vitro in Arabidopsis via the modification of the tissue sensitivity to auxin treatment. Planta 244, 231–243.
Wu, M.F., Tian, Q., Reed, J.W., 2006. Arabidopsis microRNA167 controls patterns of ARF6 and ARF8 expression, and regulates both female and male reproduction. Development 133, 4211–4218.
Zeng, X., Zeng, Z., Liu, C., Yuan, W., Hou, N., Bian, H., Zhu, M., Han, N., 2017. A barley homolog of yeast ATG6 is involved in multiple abiotic stress responses and stress resistance regulation. Plant Physiol. Biochem. 115, 97–106.
Zhang, J.Y., He, S.B., Li, L., Yang, H.Q., 2014. Auxin inhibits stomatal development through MONOPTEROS repression of a mobile peptide gene STOMAGEN in mesophyll. Proc. Natl. Acad. Sci. U.S.A. 111, E3015–E3023.